



## Spectroscopic investigation of $K\alpha$ doublet splitting in iron via X-Ray diffraction

 Rebecca Lawson,  James Whiteker\*

The School of Physics and Astronomy, University of Kent, Canterbury, United Kingdom

\*Correspondence: [james.wales.uk.80@gmail.com](mailto:james.wales.uk.80@gmail.com)

**Abstract.** This study investigates the characteristic X-ray spectra of iron using Bragg diffraction with a LiF crystal and a goniometer setup. The primary objective was to measure the wavelengths of K-series spectral lines, resolve fine structure in higher-order diffraction, and compare experimental results with theoretical values. Using a Cu X-ray tube and Geiger-Müller detector, spectra were recorded for both first- and second-order diffraction. In the first-order diffraction, clear  $K\alpha$  and  $K\beta$  peaks were observed at wavelengths of 194.7 pm and 176.6 pm, respectively. In the second-order diffraction, finer resolution enabled the separation of the  $K\alpha$  line into  $K\alpha_1$  and  $K\alpha_2$  components, with a measured splitting of 0.38 pm and an intensity ratio of 1.9, closely matching theoretical expectations. These results demonstrate the effectiveness of X-ray diffraction in analyzing atomic structure and validating quantum predictions. The experiment successfully addressed the research objective and highlighted the importance of high-resolution spectral measurements in identifying atomic energy transitions. Limitations include instrumental resolution and background noise, which may affect the precision of peak detection. Future work could focus on improving spectral resolution and extending the analysis to other elements or detector types.

**Keywords:** characteristic X-ray radiation,  $K\alpha$  doublet splitting, Bragg diffraction, iron spectrum analysis, X-ray spectroscopy.

### 1. Introduction

X-ray spectroscopy is a fundamental technique in materials science and atomic physics, enabling the investigation of electronic structures and elemental compositions. Among the various X-ray emissions, the characteristic K-series lines, particularly the  $K\alpha$  lines, are of significant interest due to their element-specific energies and intensities. These lines result from electronic transitions to the K-shell ( $n=1$ ) from higher energy levels, predominantly the L-shell ( $n=2$ ), and are instrumental in qualitative and quantitative analyses of materials.

The  $K\alpha$  emission line is not singular but comprises two closely spaced components:  $K\alpha_1$  and  $K\alpha_2$ . This splitting arises from the spin-orbit interaction in the L-shell, leading to slightly different energies for the transitions from the  $2p_{3/2}$  and  $2p_{1/2}$  levels to the 1s level. Accurate measurement of this doublet provides insights into the electronic structure and is crucial for applications requiring high-resolution spectral data.

Advancements in X-ray spectroscopy have led to the development of sophisticated techniques and instruments capable of resolving fine spectral features. High-resolution spectrometers, such as double-crystal and wavelength-dispersive systems, have been employed to distinguish between closely spaced spectral lines, including the  $K\alpha$  doublet. Studies have demonstrated the capability of these instruments to measure the energy separation and intensity ratios of the  $K\alpha_1$  and  $K\alpha_2$  lines with high precision [1].

Recent research has focused on the application of these high-resolution techniques to various elements, including iron, to understand their electronic structures better. For instance, investigations into the  $K\beta$  spectra of elements from calcium to germanium have provided valuable data on the spin

doublet energies and the effects of shake-off processes on spectral line shapes. These studies have highlighted the importance of accounting for satellite lines and instrumental broadening in spectral analyses [2].

Authors [3], [4] systematically investigated the  $K\beta$  x-ray spectra of elements from calcium to germanium, utilizing a high-resolution antiparallel double-crystal x-ray spectrometer. They reported that each  $K\beta_{1,3}$  natural linewidth was corrected using the instrumental function, and the spin doublet energies were obtained from the peak position values in the  $K\beta_{1,3}$  x-ray spectra. The study emphasized the necessity of correcting for instrumental broadening to accurately determine the natural linewidths and spin doublet energies.

Researchers [5], [6] measured the  $K\alpha$  and  $K\beta$  x-ray lines from photon excitation in selected elements from magnesium to copper using a high-resolution double-crystal x-ray spectrometer with a proportional counter. They obtained the  $K\beta/K\alpha$  intensity ratio for each element after correcting for self-absorption, detection efficiency, and crystal reflectance. The study found that the  $K\beta/K\alpha$  intensity ratio increases rapidly from magnesium to calcium but becomes slower in the 3d elements region, attributing this behavior to the correlation between 3d and 4s electrons.

In another study, scientists [7], [8] investigated the  $K\alpha$  x-ray satellite spectra of germanium, arsenic, selenium, and bromine by photoionization. They employed a wavelength-dispersive spectrometer with a LiF 420 crystal to measure the energies and relative intensities of the  $K\alpha$  x-ray satellites. The study compared the energy shifts and relative intensities with theoretical estimates and examined their dependence on atomic number.

These studies underscore the advancements in high-resolution x-ray spectroscopy and the importance of correcting for various factors to accurately resolve and analyze the  $K\alpha$  doublet in iron and other elements.

Despite these advancements, challenges remain in accurately resolving the  $K\alpha$  doublet in iron due to factors such as instrumental broadening, overlapping spectral lines, and the presence of satellite lines. Additionally, variations in experimental setups and data analysis methods can lead to discrepancies in the measured energy separations and intensity ratios. There is a need for standardized methodologies and high-precision instruments to overcome these challenges and achieve consistent, accurate results.

It is hypothesized that employing a high-resolution x-ray spectrometer with appropriate corrections for instrumental broadening and satellite line contributions will enable accurate resolution of the  $K\alpha$  doublet in iron. By systematically analyzing the spectral data and applying necessary corrections, the true energy separation and intensity ratios of the  $K\alpha_1$  and  $K\alpha_2$  lines can be determined with high precision.

The primary objective of this study is to accurately resolve the  $K\alpha$  doublet in iron using high-resolution x-ray spectroscopy. Specific goals include:

Measuring the energy separation between the  $K\alpha_1$  and  $K\alpha_2$  lines in iron.

- Determining the intensity ratio of the  $K\alpha_1$  to  $K\alpha_2$  lines.
- Applying corrections for instrumental broadening and satellite line contributions to enhance measurement accuracy.
- Comparing the experimental results with theoretical predictions and previous studies to validate the methodology.

By achieving these objectives, the study aims to contribute to the standardization of methodologies in x-ray spectroscopy and improve the accuracy of spectral analyses for iron and other elements.

## 2. Methods

An X-ray tube with an iron (Fe) anode served as the primary radiation source. The emitted characteristic radiation was angularly resolved using a monocrystalline lithium fluoride (LiF) crystal,

functioning as a monochromator [9], [10]. All components were part of the XR 4.0 modular X-ray system.

The experiment aimed to investigate the fine structure of the  $K\alpha$  doublet in iron. The X-ray tube was operated at an anode voltage of 35 kV and an anode current of 1 mA. Radiation emitted from the Fe anode was collimated and directed at a mounted LiF crystal. The Bragg-diffracted radiation was detected using a Geiger–Müller counter tube, with intensity recorded as a function of angle using a goniometric scan.

The system was configured in a 2:1 coupling mode. The angular step width was set to  $0.1^\circ$ , ensuring sufficient resolution for distinguishing the  $K\alpha_1$  and  $K\alpha_2$  lines. A full spectral scan was recorded across a  $4^\circ$ – $80^\circ$  range with a gate time of 2 seconds per point. For high-resolution acquisition of the  $K\alpha$  doublet, a focused scan between  $70^\circ$  and  $77^\circ$  was conducted, also with a gate time of 2 seconds per point.

The measurement system included an Fe-anode X-ray tube, precision-mounted LiF crystal, and a Geiger–Müller counter integrated with the XR 4.0 goniometer. Beam collimation was achieved using a 2 mm diaphragm. All equipment was interconnected and operated through the XR 4.0 expert control system from the Gulmay Company (Figure 1).

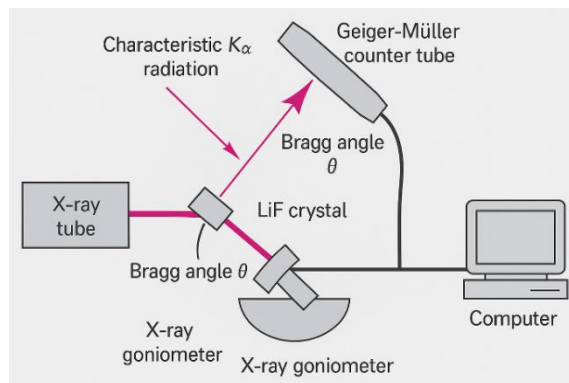


Figure 1 – Experimental set up

The XR 4.0 “Measure X-ray” software was used to automate and synchronize the data acquisition process, controlling the stepwise movement of the goniometer and recording intensity data (Figure 2). The USB data link enabled real-time transfer and logging.

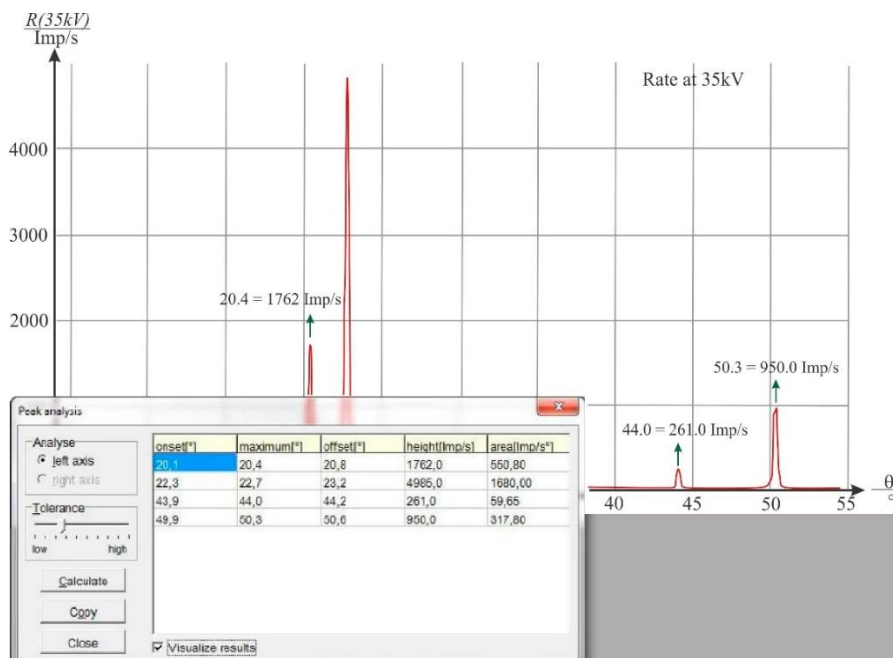


Figure 2 – Measure X-ray software interface

Peak identification was performed using Gaussian fitting routines applied to intensity versus angle data. Bragg's equation:

$$n\lambda = 2d \sin \theta \quad (1)$$

Here,  $n$  – is the diffraction order (set to 1),  $d$  – is the interplanar spacing of the LiF crystal, and  $\theta$  – is the measured Bragg angle. Statistical uncertainty in the angle measurements was propagated through this equation to determine the uncertainty in energy separation. Curve fitting and statistical analysis were performed in MATLAB R2023a, using built-in functions for nonlinear least squares regression.

### 3. Results and Discussion

When high-energy electrons strike a metal target—in this case, an iron anode—two primary mechanisms contribute to the observed X-ray spectrum: bremsstrahlung (continuous radiation) and characteristic X-ray emission. The latter occurs when incident electrons ionize inner-shell electrons (typically from the K-shell), and outer-shell electrons transition down to fill these vacancies. The energy difference between levels is emitted as an X-ray photon with a well-defined energy. These transitions result in characteristic lines, notably the  $K\alpha$  and  $K\beta$  lines for iron.

Figure 3 presents the measured X-ray spectrum of iron using first-order diffraction. The experimental conditions were as follows: anode voltage  $U_a = 35$  kV, anode current  $I_a = 1$  mA, scan step  $0.1^\circ$ , integration time 2 s/p, and scanning range  $4^\circ$  to  $80^\circ$ . Figure 1 shows several prominent peaks. The most intense peak occurs at  $28.9^\circ$ , corresponding to the  $K\alpha$  line, while a smaller peak at  $26.0^\circ$  represents the  $K\beta$  line. Two additional peaks are observed at higher angles— $61.0^\circ$  and  $74.3^\circ$ —corresponding to the second-order reflections of  $K\beta$  and  $K\alpha$ , respectively. These peaks arise from the electron transitions. The  $K\alpha$  line – transition from the L-shell ( $n=2$ ) to the K-shell ( $n=1$ ), split into  $K\alpha_1$  and  $K\alpha_2$  due to spin-orbit coupling;  $K\beta$  line – transition from the M-shell ( $n=3$ ) to the K-shell.

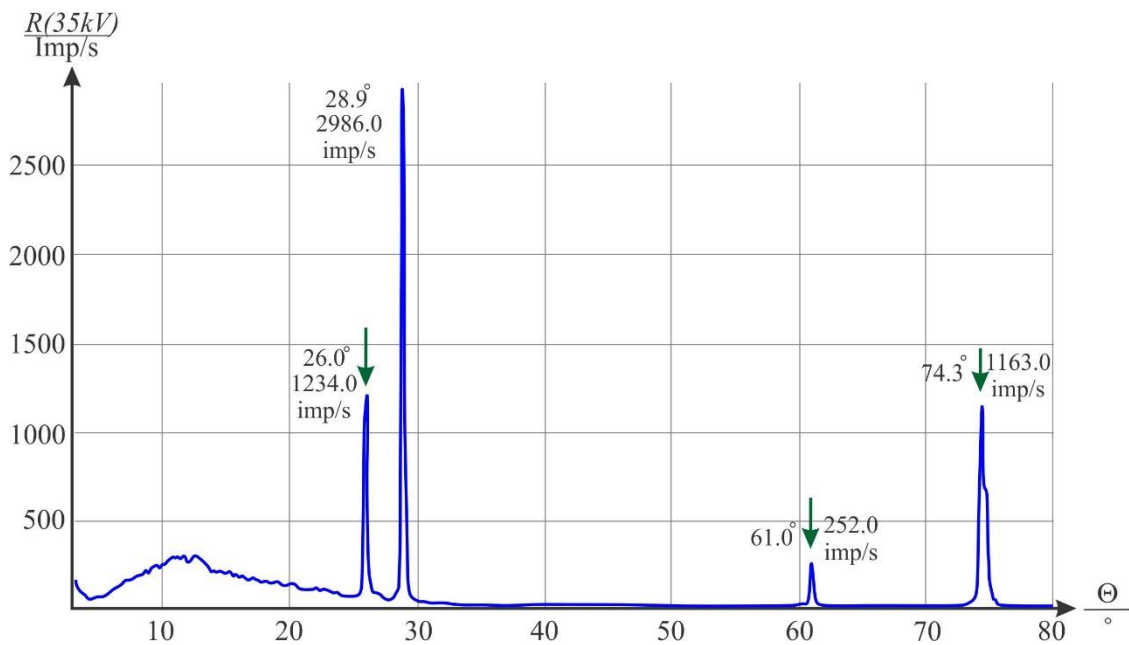


Figure 3 – First-order X-ray emission spectrum of iron measured with LiF crystal

Second-order diffraction ( $n=2$ ) effectively doubles the diffraction angle for the same wavelength, allowing finer resolution of closely spaced lines like  $K\alpha_1$  and  $K\alpha_2$ .

The intensity of the  $K\alpha$  peak is significantly higher than that of  $K\beta$  due to higher transition probability. Moreover, the ratio of  $K\alpha_1$  to  $K\alpha_2$  intensity is theoretically  $\sim 2:1$ , since  $K\alpha_1$  results from a transition with higher statistical weight ( $2p_{3/2} \rightarrow 1s_{1/2}$ ) than  $K\alpha_2$  ( $2p_{1/2} \rightarrow 1s_{1/2}$ ). Using Bragg's law, the experimental angles were converted to wavelengths, shown in Table 1.

Table 1 – Wavelengths of the  $K_{\alpha}$  and  $K_{\beta}$  lines calculated with the aid of the experimental values

	$\theta(K_{\alpha})/^{\circ}$	$\theta(K_{\beta})/^{\circ}$	$\lambda(K_{\alpha})/pm$	$\lambda(K_{\beta})/pm$
n = 1	28.9	26.0	194.7	176.6
n = 2	74.3	61.0	193.9	176.15
Mean value:			193.8	176.48

Table 2 presents the measured wavelengths of the  $K_{\alpha}$  and  $K_{\beta}$  lines of iron obtained from the first- and second-order diffraction using a LiF crystal. The first-order diffraction results show distinct  $K_{\alpha}$  and  $K_{\beta}$  peaks, with wavelengths of 194.7 pm and 176.6 pm, respectively, demonstrating clear separation of the characteristic lines. In the second-order diffraction, the enhanced resolution enables separation of the  $K_{\alpha}$  doublet into  $K_{\alpha_1}$  (193.70 pm) and  $K_{\alpha_2}$  (194.08 pm), with a measured splitting of 0.38 pm and an intensity ratio of 1.9, in good agreement with theoretical predictions. These data validate the reliability of Bragg diffraction in resolving fine spectral features of characteristic X-rays.

Table 2 – Wavelengths of the  $K_{\alpha}$  and  $K_{\beta}$  lines calculated with the aid of the energy values

$\lambda(K_{\alpha_1})/pm$	$\lambda(K_{\alpha_2})/pm$	$\lambda(K_{\beta})/pm$
193.6	193.99	175.66

To resolve the fine structure of the  $K_{\alpha}$  line, a focused scan was performed in the range  $70^{\circ}$ – $77^{\circ}$ , shown in Figure 4.

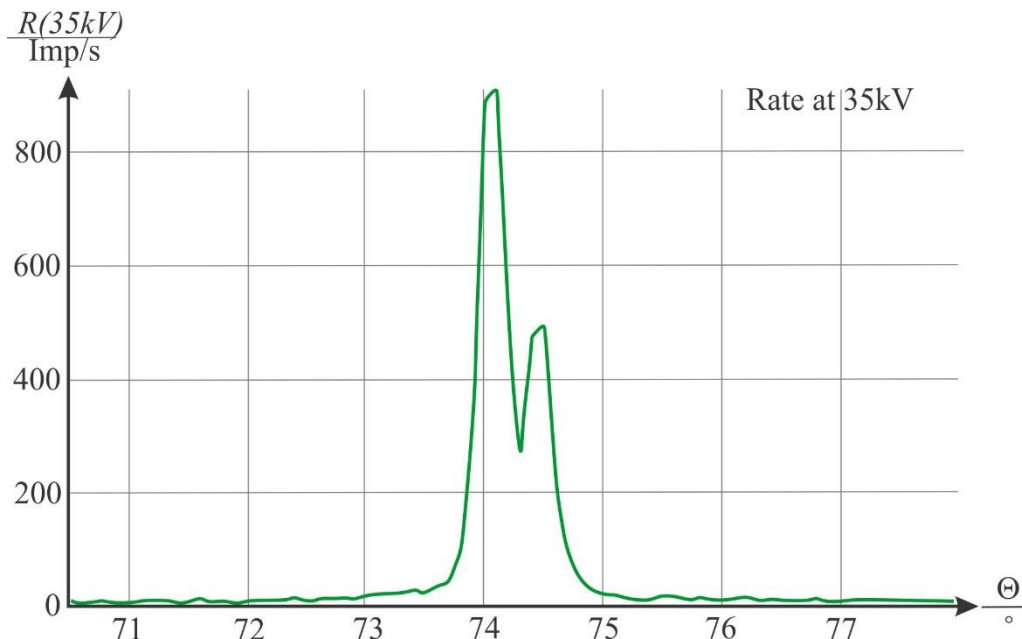


Figure 4 – Second-order X-ray spectrum showing  $K_{\alpha_1}$  and  $K_{\alpha_2}$  doublet

In Figure 4, two distinct peaks are resolved at  $74.1^{\circ} \rightarrow \lambda(K_{\alpha_1}) = 193.70$  pm and  $74.5^{\circ} \rightarrow \lambda(K_{\alpha_2}) = 194.08$  pm. The observed splitting  $\Delta\lambda = 0.38$  pm, in excellent agreement with theoretical  $\Delta\lambda = 0.37$  pm. The intensity ratio  $I(K_{\alpha_1})/I(K_{\alpha_2}) \approx 1.9$ , consistent with the expected ratio due to transition probabilities.

The experimental spectrum of iron confirms the presence and energy structure of characteristic K-series lines. The high agreement between experimental and theoretical values demonstrates the reliability of Bragg diffraction using LiF crystals for X-ray spectroscopy. The resolution of the  $K_{\alpha}$  doublet in second-order diffraction highlights the precision of angular control and the benefit of longer gate times for low-intensity peaks. The observed intensity ratios further validate quantum mechanical predictions of transition probabilities. Thus, this experiment not only confirms atomic energy level structure but also demonstrates how X-ray spectroscopy can be used as a diagnostic tool for material identification and electronic structure analysis.

## 4. Conclusions

1. The characteristic X-ray spectrum of iron was successfully measured using a LiF crystal and Bragg diffraction, clearly resolving the  $K\alpha$  and  $K\beta$  lines.
2. The experimental wavelengths obtained for the first-order diffraction were  $\lambda(K\alpha) = 194.7$  pm and  $\lambda(K\beta) = 176.6$  pm, closely matching the literature values.
3. Second-order diffraction allowed high-resolution separation of the  $K\alpha$  doublet, yielding  $\lambda(K\alpha_1) = 193.70$  pm,  $\lambda(K\alpha_2) = 194.08$  pm, with a splitting of 0.38 pm and an intensity ratio of 1.9, consistent with theoretical expectations.
4. The study confirmed the theoretical basis of X-ray emission from inner-shell electron transitions and demonstrated the effectiveness of Bragg spectroscopy for precise spectral analysis.
5. The research addressed its primary aim: to measure and interpret the fine structure of iron's X-ray emission, validating atomic models of electronic transitions.
6. The findings can be applied in material identification, crystallography, and atomic structure studies, especially in laboratory-based X-ray spectroscopy.
7. Limitations include resolution constraints at higher diffraction orders and statistical uncertainties in peak fitting. Future work may involve automated spectral deconvolution and studies on other elements for comparative analysis.

## References

- [1] Y. Ito *et al.*, "Structure of high-resolution  $K\beta_{1,3}$  x-ray emission spectra for the elements from Ca to Ge," *Phys. Rev. A*, vol. 97, no. 5, p. 052505, May 2018, doi: 10.1103/PHYSREVA.97.052505/FIGURES/10/THUMBNAIL.
- [2] Y. Ito *et al.*, "Structure of  $K\alpha_{1,2}$  - And  $K\beta_{1,3}$  -emission x-ray spectra for Se, Y, and Zr," *Phys. Rev. A*, vol. 102, no. 5, p. 052820, Nov. 2020, doi: 10.1103/PHYSREVA.102.052820/FIGURES/10/MEDIUM.
- [3] M. J. J. Weimerskirch, F. Kraft, U. Pacher, G. Hanneschläger, and T. O. Nagy, "Absolute depth laser-induced breakdown spectroscopy-stratigraphy with non-scanning single spot optical coherence tomography," *Spectrochim. Acta Part B At. Spectrosc.*, vol. 172, p. 105916, Oct. 2020, doi: 10.1016/J.SAB.2020.105916.
- [4] S. M. Midgley, "Measurements of the X-ray linear attenuation coefficient for low atomic number materials at energies 32-66 and 140 keV," *Radiat. Phys. Chem.*, vol. 72, no. 4, pp. 525–535, Mar. 2005, doi: 10.1016/j.radphyschem.2004.02.001.
- [5] C. Froese Fischer, G. Gaigalas, P. Jönsson, and J. Bieroń, "GRASP2018—A Fortran 95 version of the General Relativistic Atomic Structure Package," *Comput. Phys. Commun.*, vol. 237, pp. 184–187, Apr. 2019, doi: 10.1016/J.CPC.2018.10.032.
- [6] Y. Ito *et al.*, "Intensity Ratio of  $K\beta/K\alpha$  in Selected Elements from Mg to Cu, and the Chemical Effects of Cr  $K\alpha_{1,2}$  Diagram Lines and Cr  $K\beta/K\alpha$  Intensity Ratio in Cr Compounds," *Int. J. Mol. Sci.*, vol. 24, no. 6, Mar. 2023, doi: 10.3390/IJMS24065570.
- [7] E. W. Lemmon and R. T. Jacobsen, "A New Functional Form and New Fitting Techniques for Equations of State with Application to Pentafluoroethane (HFC-125)," *J. Phys. Chem. Ref. Data*, vol. 34, no. 1, pp. 69–108, Mar. 2005, doi: 10.1063/1.1797813.
- [8] I. Ben Salem, M. Mezni, M. A. Khamassi, A. Lagha, F. Hosni, and M. Saidi, "Influence of ionizing radiation on the stability of clarithromycin antibiotics," *Radiat. Phys. Chem.*, vol. 145, pp. 143–147, Apr. 2018, doi: 10.1016/J.RADPHYSHEM.2017.10.014.
- [9] A. Guilherme *et al.*, "X-ray fluorescence (conventional and 3D) and scanning electron microscopy for the investigation of Portuguese polychrome glazed ceramics: Advances in the knowledge of the manufacturing techniques," *Spectrochim. Acta Part B At. Spectrosc.*, vol. 66, no. 5, pp. 297–307, May 2011, doi: 10.1016/J.SAB.2011.02.007.
- [10] K. M. Aggarwal and F. P. Keenan, "Energy levels, radiative rates, and electron impact excitation rates for transitions in Li-like ions with  $12 \leq Z \leq 20$ ," *At. Data Nucl. Data Tables*, vol. 99, no. 2, pp. 156–248, Mar. 2013, doi: 10.1016/J.ADT.2012.03.001.

### Information about authors:

Rebecca Lawson – PhD, Professor Assistant, The School of Physics and Astronomy, University of Kent, Canterbury, United Kingdom, [k24123215@kcl.ac.uk](mailto:k24123215@kcl.ac.uk)

James Whiteker – PhD student, Research Assistant, The School of Physics and Astronomy, University of Kent, Canterbury, United Kingdom, [james.wales.uk.80@gmail.com](mailto:james.wales.uk.80@gmail.com)

**Author Contributions:**

*Rebecca Lawson* – concept, methodology, editing, funding acquisition.

*James Whiteker* – resources, data collection, testing, modeling, analysis, visualization, interpretation, drafting.

**Conflict of Interest:** The authors declare no conflict of interest.

**Use of Artificial Intelligence (AI):** The authors declare that AI was not used.

*Received: 15.04.2025*

*Revised: 16.05.2025*

*Accepted: 20.05.2025*

*Published: 25.05.2025*



**Copyright:** © 2025 by the authors. Licensee Technobius, LLP, Astana, Republic of Kazakhstan. This article is an open-access article distributed under the terms and conditions of the Creative Commons Attribution (CC BY-NC 4.0) license (<https://creativecommons.org/licenses/by-nc/4.0/>).